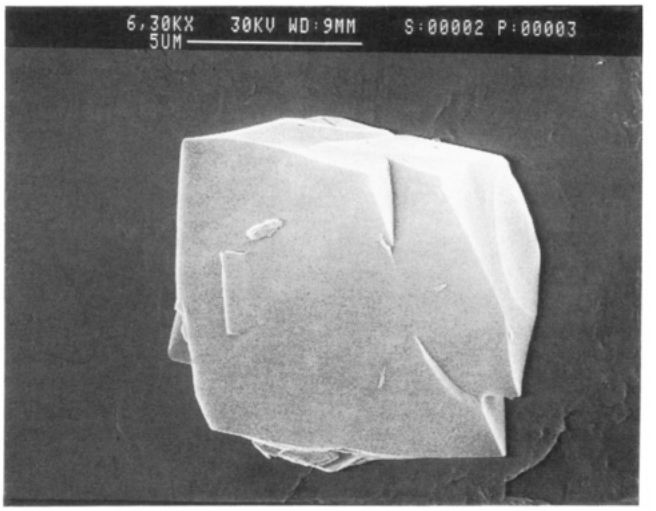

A

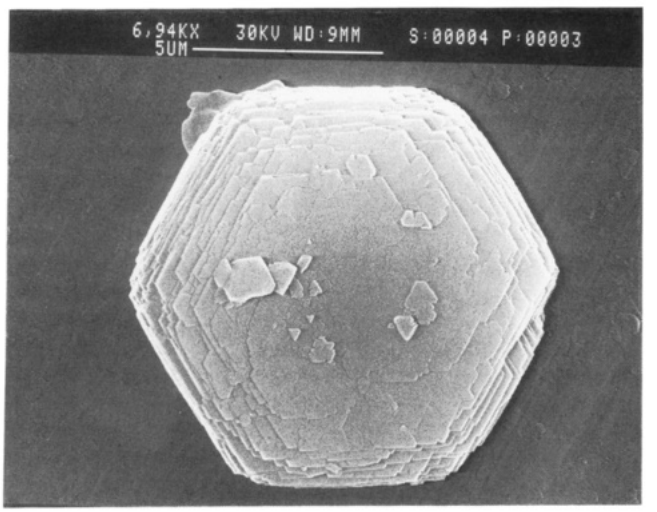

B

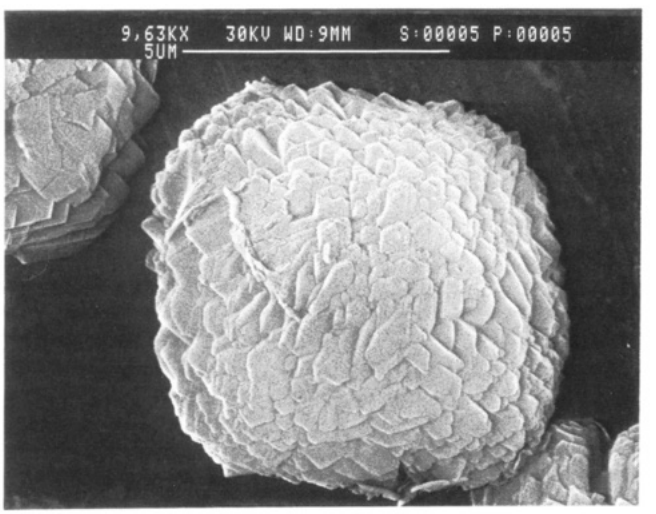

C

Figure 2. Scanning electron micrographs of samples: (A) x = 1, (B) x = 0, (C) x = 0.5. Space bar = 5 μm.

The argon adsorption data from all the samples show essentially the same isotherm in the range $10^{-5} \leq P/P_0 \leq 10^{-2}$, and the microporous adsorption capacities are listed in Table I. From these data, it is clear that there is no significant loss in adsorption capacity, indicating that there is no blocked access to portions of the crystal interiors for the intergrowth samples (x = 0.5 and 0.25).

Figure 2 shows scanning electron micrographs of the samples with x = 1, 0, and 0.5. The hex (x = 0) and FAU (x = 1) samples possess hexagonal and octahedral morphologies, respectively, as have been previously reported.[3,4] Notice that for the sample where x = 0.5, the particles are approximately 8-μm aggregates. This morphology is distinctly different from that of ZSM-20, hex, and FAU. Again, this sample does not appear to be a physical mixture of hex and FAU. Taken in total, the above data lead to the conclusion that zeolites comprised of intergrowths of cubic and hexagonal stackings of faujasite sheets can be synthesized by using mixtures of 18-crown-6 and 15-crown-5. A sample synthesized with x = 0.62 reveals an X-ray powder diffraction pattern similar to that shown for x = 0.75, while a sample synthesized with x = 0.37 gives a pattern intermediate between x = 0.25 and x = 0.5. Thus, by X-ray powder diffraction we can observe systematic changes in the hexagonal/cubic content for $0 \leq x \leq 0.5$. Variations in the hexagonal/cubic content may also occur for $x > 0.5$, but they are not observable by the techniques employed here. The use of transmission electron microscopy would certainly be advantageous in studying these materials (see Newsam et al.[6] for an example of how TEM was used to assist the structure solution of ZSM-20) and will be necessary to define domain sizes and homogeneities.

Our results are the first to show that a systematic design of intergrowth structures can occur for the faujasite system. Thus, the zeolite sample can be "tuned" to have a specific property by adjusting the synthesis conditions. It will be interesting to see if this principle can be applied to other zeolites such as zeolite beta.[11] At present, polymorphs A and B must be synthesized before this principle can be tested with zeolite-β.

Acknowledgment. We thank Dr. J. B. Higgins of the Central Research Laboratory of the Mobil Oil Company for many helpful discussions, Dr. David Young for obtaining the scanning electron micrographs, and Michael J. Annen for collecting the X-ray powder diffraction patterns.

(11) Newsam, J. M.; Treacy, M. M. J., Koetsier, W. T.; de Gruyter, C. B. *Proc. R. Soc. London A* **1988**, *420*, 375.

Synthesis of a Rotaxane via the Template Method

Charles Wu, Pierre R. Lecavalier, Ya X. Shen, and Harry W. Gibson*

Department of Chemistry
Virginia Polytechnic Institute and State University
Blacksburg, Virginia 24061

Received January 30, 1991
Revised Manuscript Received April 11, 1991

In recent years, there has been a rapid development in the area of synthesis of compounds with interesting topologies. Among these compounds, catenanes, rotaxanes, and polyrotaxanes have attracted much attention (Figure 1). The study not only reveals some interesting and im-

0897-4756/91/2803-0569$02.50/0

Scheme I

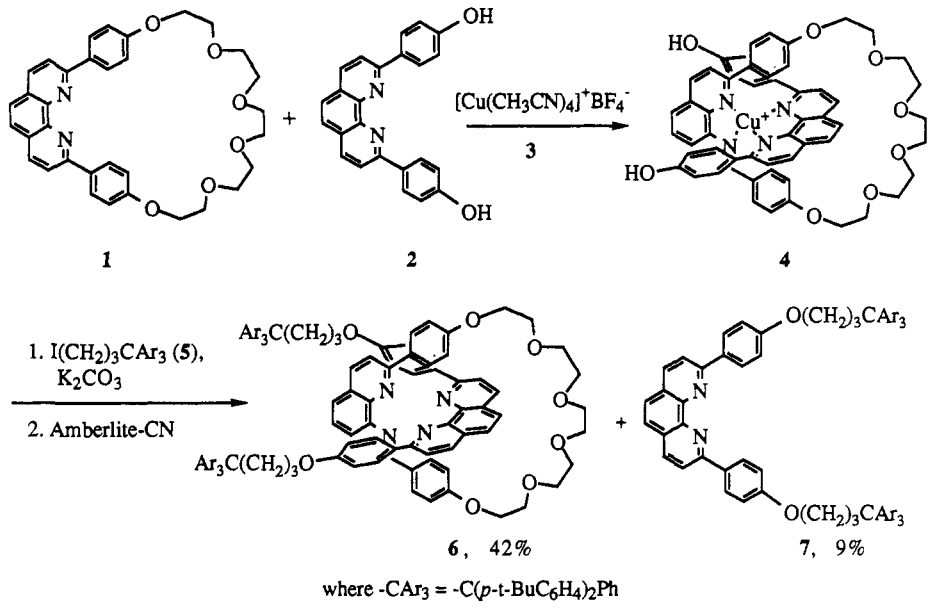

where -CAr_3 = -$C(p\text{-t-}BuC_6H_4)_2Ph$

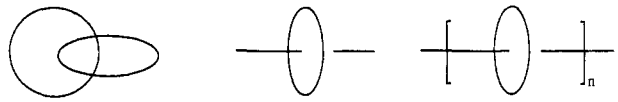

Catenane Rotaxane Polyrotaxane

Figure 1. Some topologically interesting molecular structures.

portant information about molecular architecture and intramolecular interactions but also provides us with new materials that may be used to improve interfacial bonding and blend compatibilization and as novel energy- and electron-transfer materials.

Conventionally, rotaxanes or polyrotaxanes are synthesized through the statistical threading method,[1-6] which leads to a mixture of rotaxane or polyrotaxane and unthreaded linear and cyclic compounds. Although the percentage of macrocycles in the rotaxane can be controlled by adjusting the stoichiometry of starting materials, the efficiency of threading from this method is relatively low. It is obvious that when a favorable driving force exists, the threading efficiency, and hence the yield of rotaxane and polyrotaxane, should be increased dramatically. In light of template syntheses of catenanes reported by Dietrich-Buchecker and Sauvage[7] and Stoddart et al.,[8] we decided to synthesize rotaxanes and polyrotaxanes using a similar approach. This communication will demonstrate the synthesis and characterization of the first model rotaxane compound we have obtained.

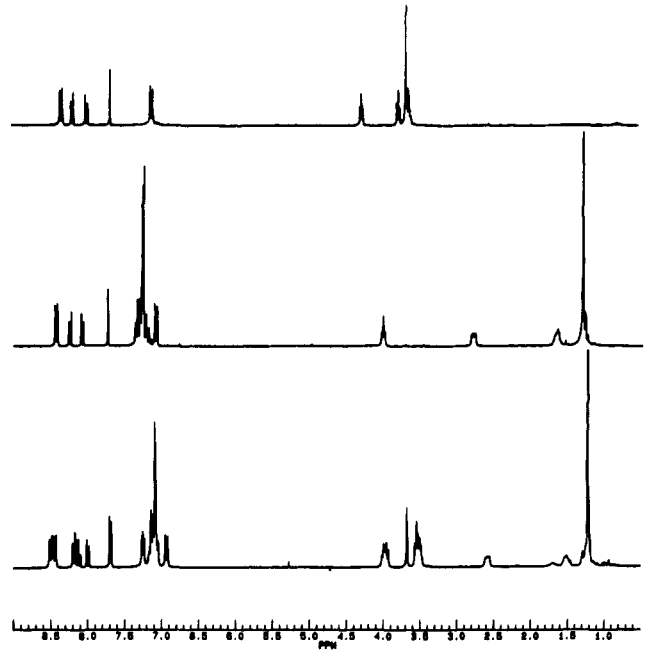

Figure 2. ^1H NMR spectra of macrocycle 1 (top), unthreaded coupling product 7 (middle), and rotaxane 6 (bottom).

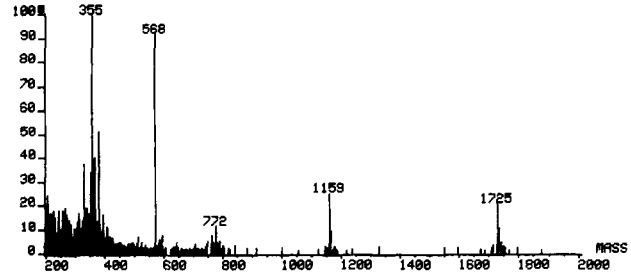

Figure 3. Mass spectrum of rotaxane 6.

Our approach to rotaxane 6 is outlined in Scheme I. Macrocycle 1 and phenanthroline-based bisphenol 2 were mixed with $[Cu(CH_3CN)_4]^+BF_4^-$ (3) in CH_2Cl_2/CH_3CN to form tetrahedral copper(I) complex 4.[7] Treatment of this complex with 5, a blocking group, in the presence of K_2CO_3

(1) Harrison, I. T.; Harrison, S. *J. Am. Chem. Soc.* **1967**, *89*, 5723.
(2) Schill, G.; Zollenkopf, H. *Nachr. Chem. Techn.* **1967**, *79*, 149.
(3) Agam, G.; Graiver, D.; Zilkha, A. *J. Am. Chem. Soc.* **1976**, *98*, 5206.
(4) Lipatova, T. E.; Kosyanchuk, L. F.; Shilov, V. V.; Gomza, Y. P. *Polym. Sci. U.S.S.R.* **1985**, *27*, 622.
(5) Lecavalier, P. R.; Engen, P. T.; Shen, Y. X.; Joardar, S.; Ward, T. C.; Gibson, H. W. *Polym. Prepr. (Am. Chem. Soc., Div. Polym. Chem.)* **1989**, *30*(1), 189. Gibson, H. W.; Bheda, M.; Engen, P. T.; Shen, Y. X.; Sze, J.; Wu, C.; Joardar, S.; Ward, T. C.; Lecavalier, P. R. *Polym. Prepr. (Am. Chem. Soc., Div. Polym. Chem.)* **1990**, *31*(1), 79.
(6) Gibson, H. W.; Bheda, M.; Engen, P. T.; Shen, Y. X.; Sze, J.; Wu, C.; Joardar, S.; Ward, T. C.; Lecavalier, P. R. *Makromol. Chem. Macromol. Symp. Vol.*, in press.
(7) Dietrich-Buchecker, C. O.; Sauvage, J.-P. *J. Am. Chem. Soc.* **1984**, *106*, 3043; *Chem. Rev.* **1987**, *87*, 795; *Angew. Chem., Int. Ed. Engl.* **1989**, *28*, 189.
(8) Ashton, P. R.; Goodnow, T. T.; Kaifer, A. E.; Reddington, M. V.; Slawin, A. M. Z.; Spencer, N.; Stoddart, J. F.; Vicent, C.; Williams, D. J. *Angew. Chem., Int. Ed. Engl.* **1989**, *28*, 1396.

Table I. Selected Chemical Shifts of Compounds 1, 6, and 7

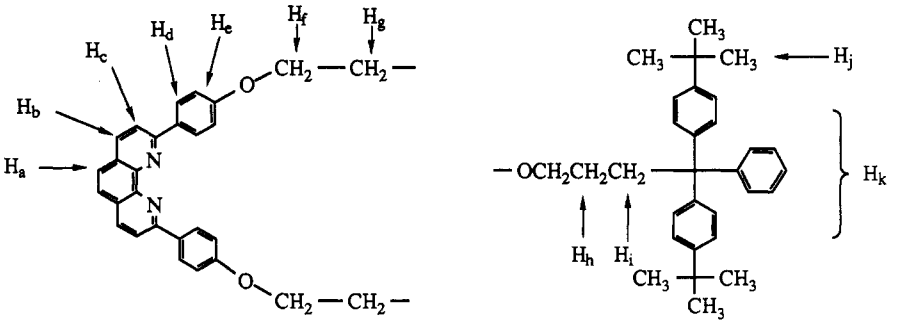

compd	H_a	H_b	H_c	H_d	H_e	H_f	H_g	H_h	H_i	H_j	H_k
1	7.65	7.98	8.17	8.33	7.10	4.25	3.92				
7	7.72	8.09	8.25	8.44	7.08			1.67	2.80	1.30	7.18–7.40
6	7.71, 7.68	8.11, 8.00	8.19	8.52, 8.45	7.15, 6.94	3.97	3.53	1.53	2.59	1.25	7.05–7.30

in DMF–CH_3CN afforded an end-capped rotaxane complex. Cu(I) ion was readily removed from the complex by the ion-exchange reaction with Amberlite–CN resin[9] to afford the free rotaxane **6**. Along with **6**, some unthreaded coupling product **7** was also obtained.

Rotaxane **6** was characterized by NMR and MS analyses. The integration of the protons shows that **6** is comprised of macrocycle **1** and coupling product **7** in 1:1 ratio; however, significant chemial shift differences have been observed between the protons on **6** and those on **1** and **7** (Figure 2). Generally speaking, shielding effects have been observed for protons on the blocking groups and on the ethyleneoxy units, and deshielding effects have been observed for protons on the phenanthroline units of the rotaxane (Table I). These data suggest that the configuration of the molecule is such that the blocking groups fall in the shielding region of the phenanthroline unit in the macrocycle, most ethyleneoxy units of the macrocycle fall in the shielding region of the linear component, and the two phenanthroline units fall in each other's deshielding region. The mass spectrum of **6** shows the fragmentation pattern expected for a rotaxane compound (Figure 3). The parent ion at m/e 1725 corresponds to the total molecular weight of the compound. The fragmentation at m/e 1159 corresponds to the linear component of the molecule, which is released when the cyclic component is broken. On the other hand, when the linear component is broken, the macrocycle is released, and this fragmentation is found at m/e 568. No fragmentation is found between m/e 1725 and 1159, indicating that no stable intermediate containing both the cyclic and the linear residues exists once the ring or the chain is broken. The elemental composition of this compound is confirmed by high-resolution MS analysis.[10]

Although rotaxane **6** has a relatively high melting point (155–158 °C), it does not crystallize from common organic solvents. Attempts to grow single crystals for X-ray crystallography studies are so far unsuccessful. Presumably the unsymmetrical triaryl blocking group on the chain has hampered the crystallization of this compound. To investigate the structure of **6**, a molecular mechanics program was used to minimize the conformational and rotational energy of the molecule. Two energy minima were obtained, where the phenanthroline units were in face–face (A) position and in face–back positions (Figure 4).[11] Interestingly, the energy of A is 32 kcal/mol lower than the energy of B according to the calculation, despite the fact that the spacing in the pentaethylenoxy portion of the ring is larger and that a face–back rotational isomer seems to be less hindered sterically. An explanation for this phenomenon is that this rotational isomer minimizes dipolar repulsions, provides the lowest dipole moment for the molecule, and hence lowers its total energy. The structure of this rotational isomer is also consistent with the ^1H NMR spectrum analysis. In both structures A and B, H_f and H_g are in the shielding region of the phenanthroline unit on the linear component. The upfield chemical shifts of 0.3–0.4 ppm indicate this strong shielding effect. The shielding effect to H_f and H_g should be much smaller for other rotational isomers. Since the chemical shifts for protons on blocking groups appeared upfield in rotaxane, the blocking groups should be in the shielding region of the macrocycle, which match with structure A. In structure B, the blocking groups are too remote from the phenanthroline unit for any shielding effect to be observed.

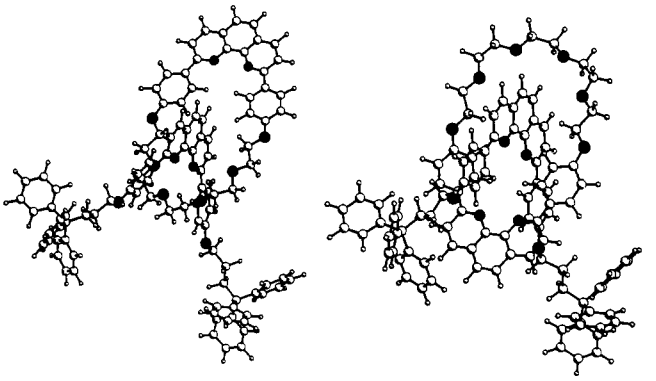

Figure 4. Molecular mechanics study of rotaxane **6** (heteroatoms are darkened).

We are currently in the process of synthesizing polyrotaxanes and other monomeric rotaxanes using similar approaches.

(9) Amberlite–Cn ion-exchange resin was prepared from Amberlite–Cl resin (Aldrich) and KCN.

(10) The high-resolution mass spectrum was obtained from Midwest Center for Mass Spectrometry using FAB analysis. Theory $C_{118}H_{123}N_4O_8$ (M + 1) 1723.9341, found 1723.9303.

(11) To simplify the calculation, a trityl group was used instead of the bis(*p-tert*-butylphenyl)phenylmethyl blocking group. This simplification should not affect the relative position of the two components at the lowest energy state. Calculations were carried out by the MM2 method using Serena Software's PCModel.

Acknowledgment. Support from the National Science Fundation Polymers Program (DMR-8712428) and the NSF Science and Technology Center for High Performance Polymeric Adhesives and Composites is gratefully acknowledged. We also acknowledge Mr. Kim C. Harich at Virginia Tech and MCMS at University of Nebraska for their help in mass spectroscopic analysis.

Registry No. 1, 90030-13-0; 2, 88498-43-5; 3, 15418-29-8; 4, 88478-97-1; 5, 134153-40-5; 6, 134153-41-6; 7, 134153-42-7.

High Potassium Ion Selectivity on Sodium-Substituted Taeniolite

Michihiro Miyake,* Toshiyuki Yoshida, Hiroaki Uchida,† Masasi Ozawa,‡ and Takashi Suzuki

Department of Applied Chemistry and Biotechnology Faculty of Engineering, Yamanashi University Takeda, Kofu 400, Japan

Received February 19, 1991
Revised Manuscript Received April 5, 1991

There are only a few inorganic cation exchangers able to efficiently separate specific cations from systems in which analogous cations coexist. For example, it is difficult to selectively take up K^+ ions in the presence of a large excess of Na^+ ions[1] although the effective ionic size of a K^+ ion in aqueous solution is different from that of a Na^+ ion. In this paper, we report the discovery of an outstanding K^+ ion sieve effect of Na-substituted taeniolite (NaT), comparing with the K^+ ion selectivity of Na-substituted hectorite (NaH) and terasilicic mica (NaTS). NaT, NaH, and NaTS, which are fluormicas, are swellable with water, and their basal spacings are 12.3 Å at 25 °C in 70% relative humidity [chemical compositions are ideally as follows: NaT, $NaMg_2LiSi_4O_{10}F_2 \cdot 2H_2O$; NaH, $Na_{1/3}Mg_{8/3}Li_{1/3}Si_4O_{10}F_2 \cdot 2H_2O$; NaTS, $NaMg_{2.5}Si_4O_{10}F_2 \cdot 2H_2O$].[2-4] The structure of taeniolite [$KMg_2LiSi_4O_{10}F_2$] is built by the stacking of the complex layer made by two SiO_4 tetrahedral sheets and one $(Mg,Li)(O,F)_6$ octahedral sheet.[5] The complex layers are connected by interlayer Na^+ ions and water molecules in NaT. Although the fundamental structures of NaT, NaH, and NaTS are similar to one another, the atomic ratios of Li/Mg in the octahedral sheet are different among them.

NaT, NaH (Topy Ind. Co.), and NaTS (Coop Chemical Ind. Co.) were repeatedly washed with distilled water, and most impurities, namely small amounts of α-cristobalite and other nonswelling particles, were removed by centrifugation prior to cation-exchange experiments. The specimens were dried at 80 °C under vacuum and stored in a desiccator with 70% relative humidity. The $Na^+ \rightleftharpoons K^+$ exchange experiments were made by the normal batch method with shaking at 25 °C, described elsewhere.[6] Each specimen of 0.1 g was equilibrated in 40 cm^3 of NaCl + KCl solution with various ratios of the two salts for 24 h in order to determine the exchange isotherms at constant total molarities of 2.5×10^{-2}, 1.0×10^{-2}, and 2.5×10^{-3} M. NaT (0.1 g) was also equilibrated in 40 cm^3 of NaCl + KCl solutions with Na^+/K^+ ratios of 10, 20, and 30 at K^+ ion concentrations of 200, 300, 400, and 500 ppm for 24 h in order to further clarify K^+ ion selectivity in the presence of a large excess of Na^+ ions. After the reaction, the solid and solution phases were separated by centrifugation, and an aliquot of supernatant was collected for chemical analyses. The solutions were analyzed for Li, Na, and K by atomic absorption spectroscopy. At least three replications were carried out in the cation-exchange experiments with concurrent results.

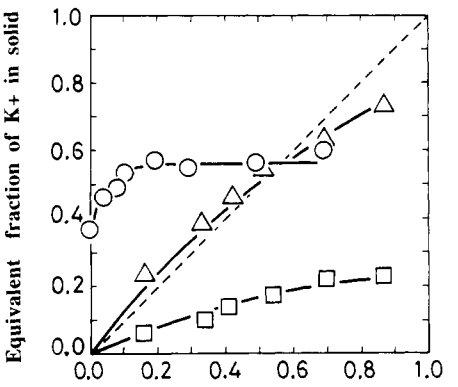

Figure 1. $Na^+ \rightleftharpoons K^+$ exchange isotherms on NaT (○), NaH (△), and NaTS (□) at a constant total molarity of 1.0×10^{-2} M.

The exchange reaction of NaT, NaH, and NaTS of 1 g with 1.0×10^{-2} M KCl solutions attained steady states within 24 h, and the molar ratios of Na^+/K^+ during the reactions were found to be close to 1.0. The interlayer Na^+ ions of ca. 55% in NaT, 75% in NaH, and 25% in NaTS, whose theoretical cation exchange capacities are 235, 78, and 233 mequiv/100 g, respectively, were exchanged for K^+ ions at an equilibrium state. The cation exchanges that occurred were incomplete. This was considered to be due to the fact that it is impossible to synthesize solid solutions between Na and K substitutions over the entire composition range.[7]

The exchange isotherms on NaT, NaH, and NaTS at a constant total molarity of 1×10^{-2} M are shown in Figure 1. The $Na^+ \rightleftharpoons K^+$ exchange process on mica is represented by

$$K^+ + \text{Na mica} \rightleftharpoons Na^+ + \text{K mica}$$

K^+ ions are preferable to Na^+ ions if the exchange isotherm lies above the diagonal line, whereas Na^+ ion are preferable to K^+ ions if the exchange isotherm lies below the diagonal line, and the diagonal line represents no preference between these ions.[8] The $Na^+ \rightleftharpoons K^+$ exchange isotherm on NaT rises steeply and attains a plateau above the diagonal line in the initial stages, which reveals that K^+ ions are extremely preferred over Na^+ ions in the low-concentration region of K^+ ions. The $Na^+ \rightleftharpoons K^+$ exchange isotherm on NaH lies just above the diagonal line in the low-concentration region of K^+ ions, which reveals that K^+ ions are moderately preferred over Na^+ ions. The $Na^+ \rightleftharpoons K^+$ exchange isotherm on NaTS lies below the diagonal line over the concentration range, which reveals that Na^+ ions are preferred over K^+ ions. The order of K^+ ion selectivity was, therefore, concluded to be NaTS < NaH ≪ NaT in

† Present address: Oki Electric Co., Ltd, Tokyo, Japan.
‡ Present address: Nippon Kemikon Co., Ltd, Tokyo, Japan.

(1) Suzuki, T.; Miyake, M.; Yoshikawa, Y.; Yoshida, T. *Bull. Soc. Seawater Sci. Jpn.* **1990**, *44*, 185–188.
(2) Kitajima, K.; Sugimori, K.; Daimon, N. *J. Chem. Soc. Jpn.* **1973**, 1885–1892.
(3) Kitajima, K.; Daimon, N. *J. Chem. Soc. Jpn.* **1974**, 685–689.
(4) Kitajima, K.; Daimon, N. *J. Chem. Soc. Jpn.* **1975**, 991–995.
(5) Toraya, H.; Iwai, S.; Marumo, F.; Hirao, M. *Z. Kristallogr.* **1977**, *146*, 73–83.
(6) Suzuki, T.; Hatsushika, T.; Miyake, M. *J. Chem. Soc., Faraday Trans. 1*, **1982**, *78*, 3605–3611.
(7) Kondo, R.; Daimon, M.; Asaga, K.; Nishikawa, T.; Kitajima, K.; Daimon, N. *J. Am. Ceram. Soc.*, **1980**, *63*, 41–43.
(8) Rees, L. V. C. *The Properties and Applications of Zeolites*; The Chemical Society: London, 1979; pp 218–243.

0897-4756/91/2803-0572$02.50/0